THE JOURNAL OF BIOLOGICAL CHEMISTRY VOL. 280, NO. 40, pp. 34056–34062, October 7, 2005
Printed in the U.S.A.

Anthrax Biosensor, Protective Antigen Ion Channel Asymmetric Blockade*

Received for publication, July 20, 2005 Published, JBC Papers in Press, August 8, 2005, DOI 10.1074/jbc.M507928200

Kelly M. Halverson[‡], Rekha G. Panchal[§], Tam L. Nguyen[§], Rick Gussio[§], Stephen F. Little[‡], Martin Misakian[¶], Sina Bavari[‡], and John J. Kasianowicz[‖1]

From the [‡]United States Army Medical Research Institute of Infectious Diseases, Fort Detrick, Frederick, Maryland 21702-5011, [§]Developmental Therapeutics Program, Target Structure-based Drug Discovery Group, National Cancer Institute-Science Applications International Corporation, Frederick, Maryland 21702, [¶]National Institute of Standards and Technology, Electronics and Electrical Engineering Laboratory, Gaithersburg, Maryland 20899-8172, and [‖]National Institute of Standards and Technology, Advanced Chemical Sciences Laboratory and the Electronics and Electrical Engineering Laboratory, Semiconductor Engineering Division, Gaithersburg, Maryland 20899-8120

The significant threat posed by biological agents (*e.g.* anthrax, tetanus, botulinum, and diphtheria toxins) (Inglesby, T. V., O'Toole, T., Henderson, D. A., Bartlett, J. G., Ascher, M. S., Eitzen, E., Friedlander, A. M., Gerberding, J., Hauer, J., Hughes, J., McDade, J., Osterholm, M. T., Parker, G., Perl, T. M., Russell, P. K., and Tonat, K. (2002) *J. Am. Med. Assoc.* 287, 2236–2252) requires innovative technologies and approaches to understand the mechanisms of toxin action and to develop better therapies. Anthrax toxins are formed from three proteins secreted by fully virulent *Bacillus anthracis*, protective antigen (PA, 83 kDa), lethal factor (LF, 90 kDa), and edema factor (EF, 89 kDa). Here we present electrophysiological measurements demonstrating that full-length LF and EF convert the current-voltage relationship of the heptameric PA_{63} ion channel from slightly nonlinear to highly rectifying and diode-like at pH 6.6. This effect provides a novel method for characterizing functional toxin interactions. The method confirms that a previously well characterized PA_{63} monoclonal antibody, which neutralizes anthrax lethal toxin in animals *in vivo* and *in vitro*, prevents the binding of LF to the PA_{63} pore. The technique can also detect the presence of anthrax lethal toxin complex from plasma of infected animals. The latter two results suggest the potential application of PA_{63} nanopore-based biosensors in anthrax therapeutics and diagnostics.

Similar to other A-B binary toxins, the putative mechanism of anthrax toxin-induced toxinemia suggests that the B-protein, protective antigen (PA),[2] binds to a cell surface receptor (2, 3) and is subsequently cleaved at the N terminus into two fragments, PA_{20} and PA_{63} (4, 5). Following cleavage, PA_{63} oligomerizes into a heptameric prepore on the cell membrane (6). The A-proteins, lethal factor (LF) and edema factor (EF), competitively bind to the heptameric PA_{63}, forming the $(PA_{63})_7$-LF/EF complex which is endocytosed (7). Upon acidification of the endosome, the heptameric PA_{63} is thought to undergo a conformational change, insert into the membrane, and form a functional transmembrane pore. In this model, LF and EF are subsequently translocated across the endosomal membrane into the cytosol (8). Determining the mechanism of PA_{63}-mediated translocation of EF/LF into the cytosol remains an interesting challenge. Here we present proof-of principle for a potential biosensor in anthrax diagnostics and therapeutics.

EXPERIMENTAL PROCEDURES

Proteins—Purified PA_{63}, LF, and EF proteins (List Biological Laboratories Inc.) from *Bacillus anthracis* were used for these studies.

Antibody—Hybridoma PA_{63} 1G3–1-1 was prepared by fusing spleen cells from female BALB/c mice injected with PA_{63} with SP2/O-Ag 14 myeloma cells and subcloning positive hybridomas twice by limiting dilution (9, 10). Ascites was produced in BALB/c female mice and was clarified by centrifugation. This ascites monoclonal antibody, 1G3–1-1, prevents binding of LF to PA_{63} through steric hindrance (9).

Electrophysiology—Channel recordings were carried out with planar lipid bilayer membranes as previously described (11). Briefly, solvent-free diphytanoyl phosphatidylcholine membranes were formed on a 50–100-μm diameter hole in a thin Teflon partition. The partition separated two identical Teflon chambers that each contained ~2 ml of aqueous solution (0.1 M KCl, 5 mM MES, pH 6.6). Voltage was applied across the membrane via Ag-AgCl electrodes. The current was amplified using a patch-clamp instrument (Axon Instruments 200B), recorded with an analog to digital converter (Axon Instruments Digi-Data 1322), and analyzed off-line. A negative transmembrane potential drove anions from the *cis* to the *trans* chamber. Details of this particular method were summarized elsewhere (12).

Channels were formed by adding small aliquots (~100 ng) of the purified PA_{63} to the aqueous electrolyte solution bathing one side of the membrane (herein called *cis*). The formation of individual channels was indicated by the stepwise increases in ionic current monitored at +50 mV applied potential. During recording of the ionic current in the steady-state experiments, the membrane potential was held constant at either +50 or +100 mV. To determine the instantaneous current-voltage (*I-V*) relationships, we generated current by applying brief (0.5 s) voltage pulses (typically +200 to −200 mV in 10-mV steps) across the membrane and averaged the first 100 ms of the signal to obtain the instantaneous (*I-V*) relationship.

Collection of Plasma from Infected Animals and Purification of the $(PA_{63})_7$-LF Complex—The $(PA_{63})_7$-LF complex was purified from the plasma of infected guinea pigs. Research was conducted in accordance with the Animal Welfare Act and other statutes and regulations relating

* This work was supported in part by the Medical Biological Defense Research Program, the U. S. Army Medical Research Institute of Infectious Diseases (USAMRIID Research Plan 02-4-2C-012), the National Institute of Standards and Technology (NIST) Advanced Technology Program, the NIST "Single Molecule Manipulation and Measurement" program, Defense Advanced Research Projects Agency, and the National Science Foundation (NIRT Grant CTS-0304062). The costs of publication of this article were defrayed in part by the payment of page charges. This article must therefore be hereby marked "*advertisement*" in accordance with 18 U.S.C. Section 1734 solely to indicate this fact.

[1] To whom correspondence should be addressed: National Institute of Standards and Technology, Technology Bldg. 225, Rm. B326, Gaithersburg, MD 20899-8120. Tel.: 301-975-5853; Fax: 301-948-4081; E-mail: john.kasianowicz@nist.gov.

[2] The abbreviations used are: PA, protective antigen; LF, lethal factor; EF, edema factor; *I-V*, current voltage; MES, 4-morpholineethanesulfonic acid.

Report Documentation Page

Form Approved
OMB No. 0704-0188

1. REPORT DATE	2. REPORT TYPE	3. DATES COVERED
7 OCT 2005	**N/A**	**-**

4. TITLE AND SUBTITLE	5a. CONTRACT NUMBER
Anthrax biosensor: protective antigen ion channel asymmetric blockade, Journal of Biological Chemistry 280:34056 - 34062	5b. GRANT NUMBER
	5c. PROGRAM ELEMENT NUMBER
6. AUTHOR(S)	5d. PROJECT NUMBER
Halverson, KM Panchal, RG Nguyen, TL Gussio, R Little, SF Bavari, S Kasianowicz, JJ	5e. TASK NUMBER
	5f. WORK UNIT NUMBER
7. PERFORMING ORGANIZATION NAME(S) AND ADDRESS(ES)	8. PERFORMING ORGANIZATION REPORT NUMBER
United States Army Medical Research Institute of Infectious Diseases, Fort Detrick, MD	**RPP-05-403**
9. SPONSORING/MONITORING AGENCY NAME(S) AND ADDRESS(ES)	10. SPONSOR/MONITOR'S ACRONYM(S)
	11. SPONSOR/MONITOR'S REPORT NUMBER(S)

12. DISTRIBUTION/AVAILABILITY STATEMENT

Approved for public release, distribution unlimited

13. SUPPLEMENTARY NOTES

The original document contains color images.

14. ABSTRACT

Bacillus anthracis secretes three proteins (protective antigen, PA; lethal factor, LF; and edema factor, EF) that are the basis for anthrax infection. We present electrophysiological measurements that demonstrate the effect of full-length LF and EF on ion channels formed by the proteolytically activated species of PA (PA63) in planar lipid bilayer membranes. LF and EF convert the heptameric PA63 channel current-voltage relationship from slightly nonlinear to one that is highly rectifying and diode-like at pH 6.6. This striking effect provides an innovative method for characterizing functional toxin interactions and can be applied as an anthrax therapeutic biosensor.

15. SUBJECT TERMS

Bacillus anthracis, anthrax, protective antigen, lethal factor, edema factor, PA, LF, EF, ion channel, biosensor

16. SECURITY CLASSIFICATION OF:			17. LIMITATION OF ABSTRACT	18. NUMBER OF PAGES	19a. NAME OF RESPONSIBLE PERSON
a. REPORT	b. ABSTRACT	c. THIS PAGE			
unclassified	**unclassified**	**unclassified**	**SAR**	**7**	

Standard Form 298 (Rev. 8-98)
Prescribed by ANSI Std Z39-18

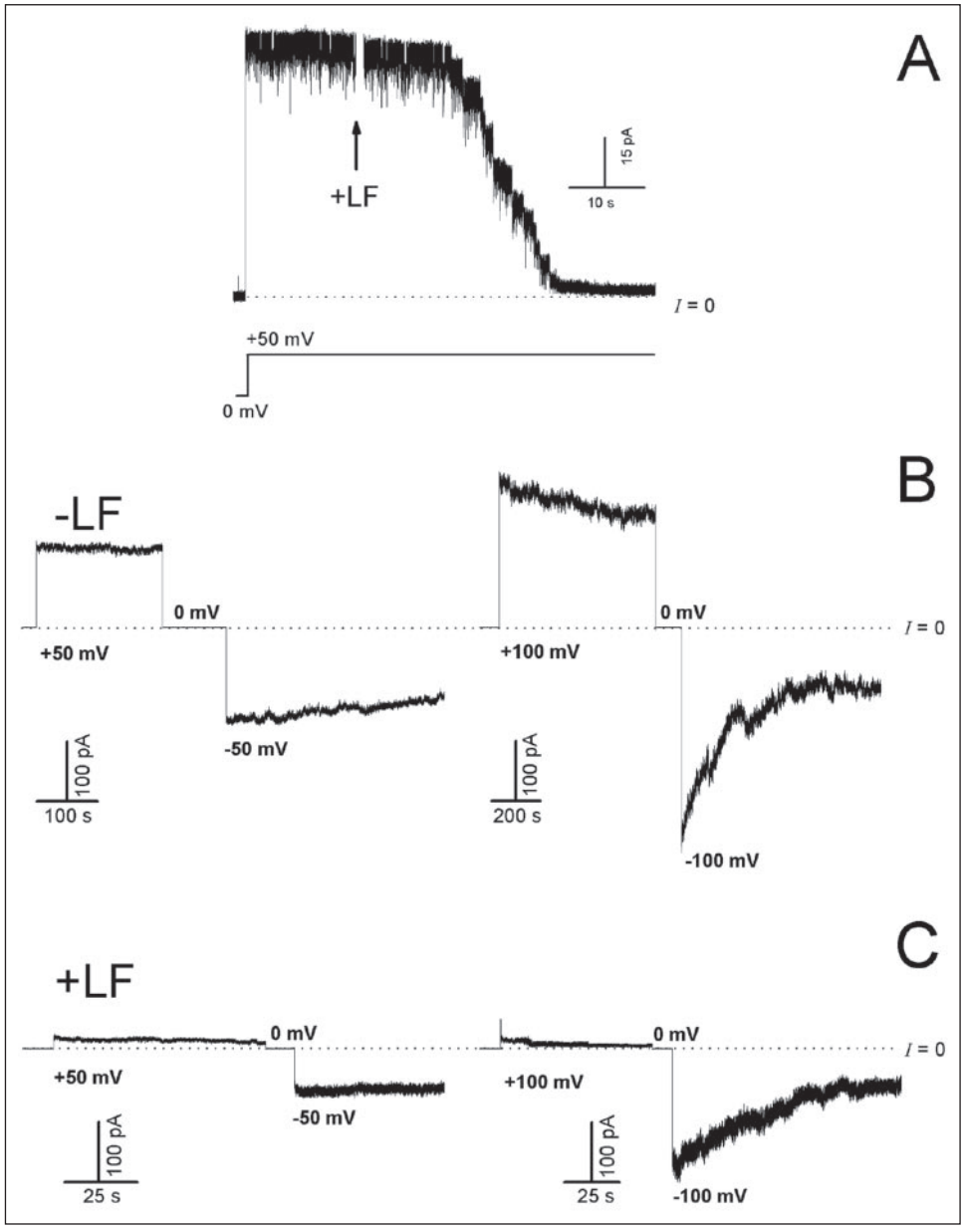

FIGURE 1. *A*, lethal factor decreases the conductance of PA_{63} channels reconstituted in a planar bilayer membrane. The method for membrane formation and ionic current recording was described elsewhere (12). In the absence of LF, there was a persistent ionic current through ~14 PA_{63} channels. The addition of 3 nM LF to the same side of the chamber (*cis*) that PA_{63} was added caused the current to decrease. Each downward step corresponds to the virtually complete blockade of individual channels. The *dashed line* indicates zero current. The solutions on both sides of the membrane contained 0.1 M KCl, 5 mM MES, pH 6.6, and the applied potential was +50 mV. *B* and *C*, the LF-induced blockade of voltage-gated PA_{63} channels is reversed by negative applied potential. In the absence of LF (*B*), the PA_{63} ionic current spontaneously decreases over several min. The decrease in current is more rapid for greater magnitudes of the applied potential and for negative voltages. *C*, the addition of 3 nM LF blocks virtually all the ionic current for positive potentials. In contrast, some current flows for negative applied potentials. In *panels B* and *C*, the membrane contained ~ 36 PA_{63} channels.

to animals and experiments involving animals and adheres to principles stated in the Guide for the Care and Use of Laboratory Animals (NRC 1996) in facilities that are fully accredited by the Assesssment and Accreditation of Laboratory Animal Care, International. Infected animals that appeared moribund were anesthetized, and blood was drawn into tubes containing EDTA to inhibit cleavage of PA_{83} by serum proteases. Blood samples were mixed, centrifuged, and filtered through a 0.2-μm filter and stored at −70 °C. Approximately 0.25 ml of the sample (diluted 1:1 with phosphate-buffered saline) was loaded on a Superose 6 size exclusion column (Amersham Biosciences) previously equilibrated with phosphate-buffered saline, pH 7.4. LF activity in the different fractions collected was determined by fluorescent plate-based assay as previously described (13) and briefly summarized below. The peak fraction corresponding to the $(PA_{63})_7$-LF complex and exhibiting LF activity was used for electrophysiological studies.

Fluorescent-based Kinetic Assay—Known concentrations of serially diluted free LF or unknown concentrations of complexed LF were incubated with 20 μM optimized peptide substrate (13). Kinetic measurements were made every minute for 30 min using a fluorescence plate reader (Tecan Safire). The peptide has an excitation peak at 324 nm and an emission peak at 395 nm. A calibration curve was established using free LF as a standard. The complexed LF concentration was determined using the standards. The concentration of complexed LF was also confirmed by enzyme-linked immunosorbent assay as described previously (14).

RESULTS AND DISCUSSION

Fig. 1*A* shows an ionic current recording for 14 PA_{63} channels (~3.8 pA/channel for an applied potential $V = +50$ mV) in a planar phospholipid bilayer membrane. The introduction of LF (~3 nM) causes a rapid and virtually complete reduction in PA_{63} channel current as revealed by the stepwise decrements (Fig. 1*A*). Previous reports at pH 6.6 and 5.5 suggested that various factors, such as tetraalkylammonium ions and the N-terminal binding fragments of both EF and LF (*i.e.* EF_N and LF_N), can cause a decrease in the PA_{63} channel conductance (15–19). In these earlier studies, the ionic current blockades were removed by greater

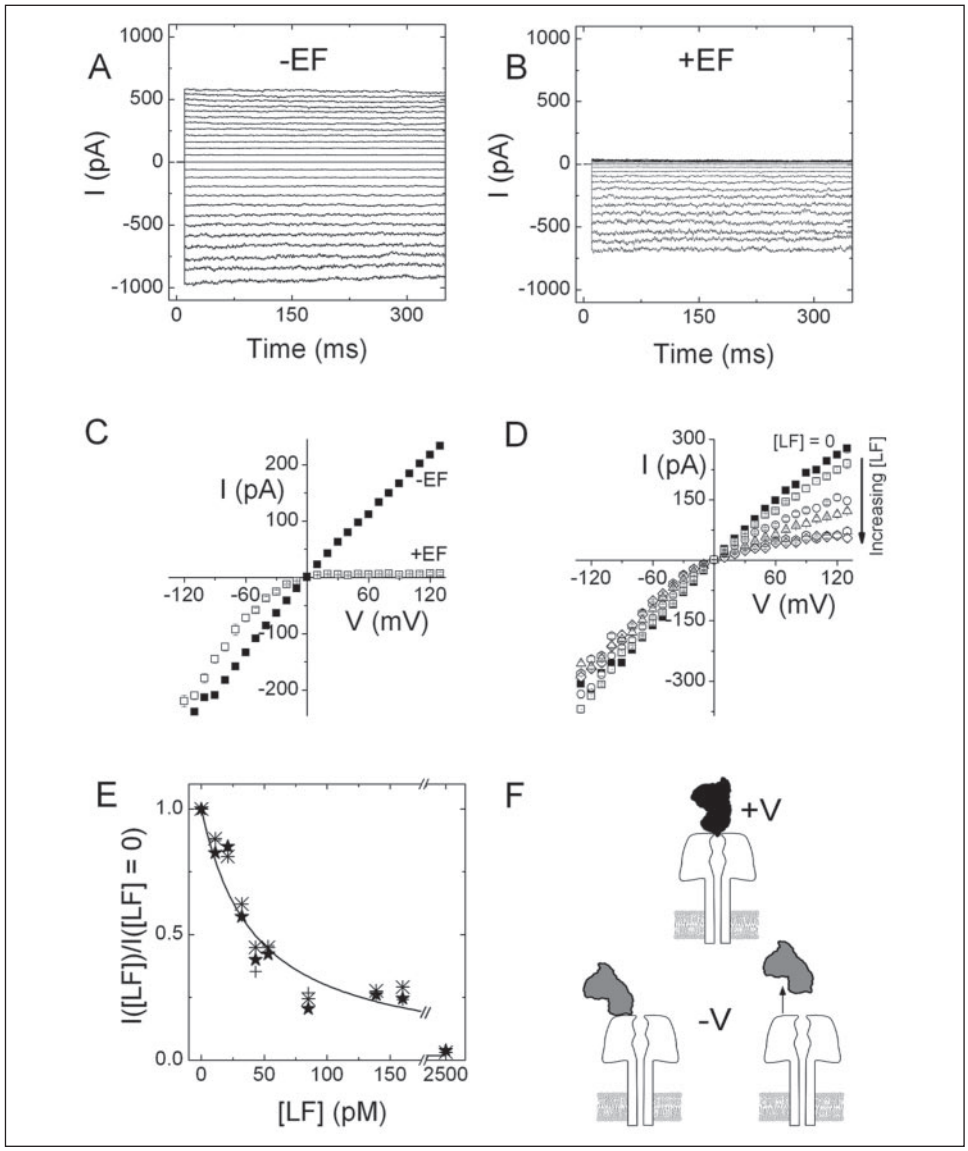

FIGURE 2. **The apparent dissociation constant for EF and LF binding to PA_{63} ion channels estimated from instantaneous *I-V* relationships.** The ionic current *versus* time for PA_{63} channels in the absence (*A*) and presence (*B*) of EF (~2.5 nM). The current is caused by short voltage pulses (~500-ms duration) that varied from +120 to −120 mV in 10-mV increments (short-lived capacitance current artifacts are not shown). EF blocks PA_{63} channels much more effectively for positive applied potentials. *C*, the instantaneous *I-V* relationship of PA_{63} channels alone (*filled squares*) and in the presence of ~3 nM EF (*open squares*). The current is generated by short voltage pulses that varied from +130 to −130 mV. *D*, the instantaneous current-voltage relationship of PA_{63} channels in the presence of different concentrations of LF. LF = 0, *filled squares*; 11 pM, *open squares*; 32 pM, *open circles*; 53 pM, *open triangles*; 85 pM, *open hexagons*; and 160 pM, *open diamonds*. The current is caused by short voltage pulses (~500-ms duration) that varied from +130 to −130 mV in 10-mV increments. *E*, the ratio of the ionic current in the presence of LF to that in its absence as a function of LF concentration for three different values of the applied potential (+50 mV, *filled stars*; +100 mV, *crosses*; and +130 mV, *asterisks*). The *solid line* through the data is the result of a least-squares fit of an equation to the data that assumes 1 LF binds to 1 PA_{63} channel (see "Results and Discussion"). The result suggests that the apparent dissociation constant for the binding of LF to PA_{63} is ~50 pM. The buffer in both the *cis* and *trans* chambers for each panel was 0.1 M KCl, 5 mM MES at pH 6.6. *F*, a schematic diagram depicting a PA_{63} channel with a single LF (*gray* or *black*) bound to describe the ionic current rectification caused by LF and EF. The *top panel* depicts LF blocking the channel by a positive applied potential (+*V*). The *bottom panel* depicts LF pushed out of the PA_{63} channel entrance or completely separated from PA_{63} by a negative applied potential (−*V*).

transmembrane voltages (16–19). For instance, voltages greater than +40 mV increased PA_{63} channel conductance at pH 5.5 following the blockade by LF_N (19). However, although no data were shown, the authors state that current blockade relief is not seen at pH 6.6 for LF_N. Interestingly, this is exactly the case for the full-length LF-induced blockade that we report here at pH 6.6 (see Figs. 1 and 2 and below).

In the absence of LF (Fig. 1*B*), the current through many PA_{63} channels decreases relatively slowly, and this gating effect is voltage dependent (16, 17). The greater the magnitude of the applied potential, the more rapidly the channels gate to lesser conductance states. In addition, the current decays more rapidly for negative potentials than for positive voltages of the same magnitude (Fig. 1*B*). In the presence of LF (Fig. 1*C*), the blockade of PA_{63} channel conductance is highly asymmetric with respect to the sign of the transmembrane potential. That is, the ionic current is virtually nonextant for positive potentials, whereas negative voltages (*i.e.* −50 and −100 mV) produce significant current through the PA_{63} channels even in the presence of LF. In contrast, LF added to the *trans* chamber had no effect on the PA_{63} conductance for either sign of the potential (data not shown). In addition, LF had no effect on channels formed by the pore-forming toxin *Staphylococcus aureus* α-hemolysin (data not shown). These experiments demonstrate that the creation of a rectifying ion channel by LF binding to the cap domain of PA_{63} is not only site specific but also pore-forming toxin specific. Similar results were observed for EF binding to the channel formed by PA_{63}.

The intrinsic gating of the PA_{63} channel (Fig. 1*B*) makes accurate determination of LF-$(PA_{63})_7$ or EF-$(PA_{63})_7$ binding parameters difficult. However, measuring the PA_{63} instantaneous *I-V* relationship, without and with either LF or EF, avoids that issue. In particular, several hundred ms-long voltage pulses (*e.g.* +120 to −120 mV, in 10-mV steps) are applied across the membrane in the absence or presence of ~2.5 nM EF (Fig. 2, *A* and *B*, respectively). EF binding to the PA_{63} channel changes the *I-V* relationship from slightly nonlinear to strongly rectifying, as was observed for full-length LF (13). Note that EF causes virtually complete extinction of the ionic current only for positive voltages. The *I-V* relationship for a similar experiment is shown in Fig. 2*C*. These functional measurements and the analysis below demonstrate that the interaction between $(PA_{63})_7$ and EF or LF cannot be described as merely a passive block of the PA_{63} ion channel. In fact, the LF-induced blockade of PA_{63}-mediated tracer ion flux into and out of Chinese hamster ovary-CK1 cells as demonstrated by Zhao *et al.* (20) supports our conclusion that LF and EF bind strongly to PA_{63} channels and notably decrease PA_{63} ionic conductance for even small positive potentials (Fig. 2*B* and Ref.

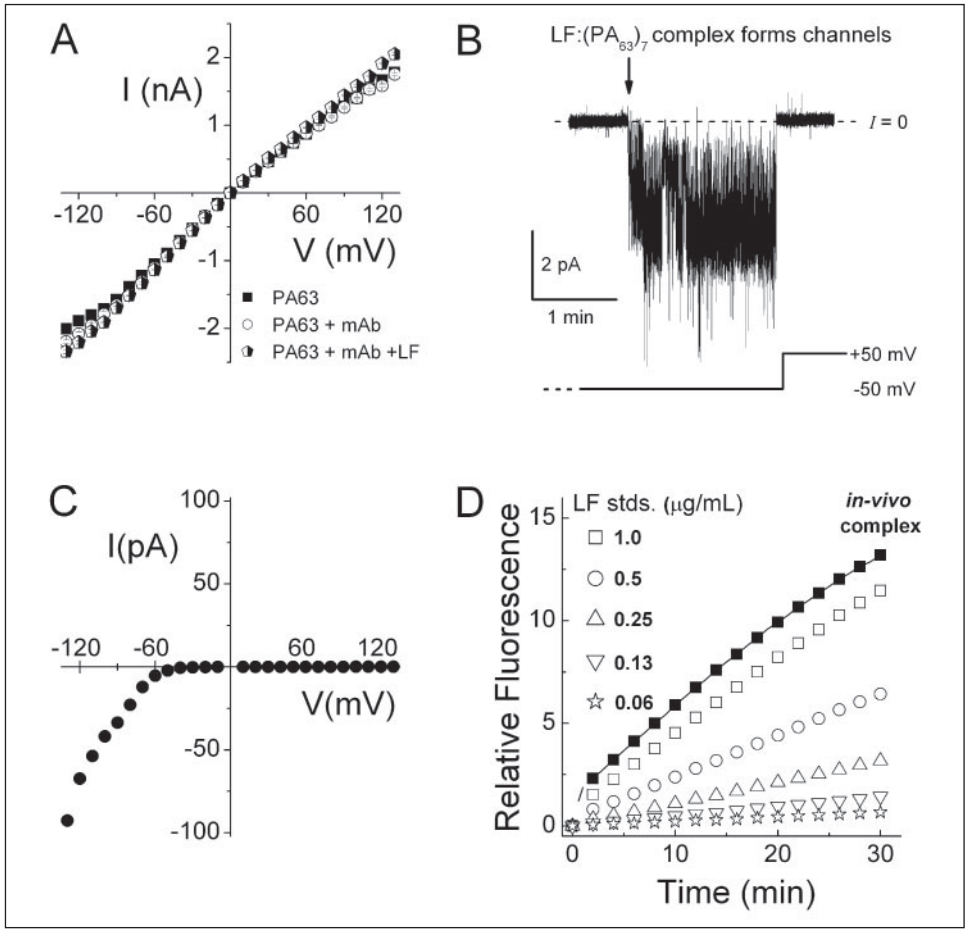

FIGURE 3. **The $(PA_{63})_7$ ion channel as a rapid diagnostic anthrax biosensor.** *A*, application as a therapeutic screen demonstrated by inhibition of LF binding to the PA_{63} channels. The instantaneous *I-V* relationship of PA_{63} channels (*filled squares*), PA_{63} channels in the presence of a monoclonal antibody (1G3–1-1) (*open circles*), and PA_{63} channels with the monoclonal antibody bound followed by the addition of ~3 nM LF (*half-filled pentagons*). *B* and *C*, use of the method as a diagnostic tool to detect anthrax lethal toxin. *B*, lethal toxin (the complex of LF and $(PA_{63})_7$) purified from the serum of a guinea pig infected with fully virulent *B. anthracis* spontaneously forms rectifying channels. The concentration of LF in the complex with $(PA_{63})_7$ in the chamber is ~30 pM. *C*, typical *I-V* relationship for the lethal toxin complex demonstrates that lethal toxin (~60 nM LF in the complex with $(PA_{63})_7$) formed *in vivo* is detectable with our method. *D*, the concentration and activity of LF in the complex determined with a fluorescence-based kinetic assay. The enzymatic activity of free LF at different concentrations was measured directly (*open symbols*). A calibration curve derived from these LF standards is used to determine the concentration of LF bound to the PA_{63} channel in serum (*filled squares*).

14). Our electrophysiological results (Figs. 1 and 2) demonstrate that both full-length LF and EF markedly occlude PA_{63} ion conductance only at positive applied potentials. The block may persist for zero transmembrane potential.

The effect shown in Fig. 2*B* provides a method to probe the interaction between EF or LF and the PA_{63} channel. Fig. 2*D* illustrates the *I-V* relationships for PA_{63} channels in the absence of LF and for five different concentrations of LF. For increasing [LF] and $V > 0$, the instantaneous current decreases markedly with respect to that for [LF] = 0. In contrast, for $V < 0$, LF has only a slight effect on the instantaneous current. The ratio of the current in the presence of LF to that in the absence of LF for $0 \leq [LF] \leq 2.5$ nM for three different positive applied potentials is shown in Fig. 2*E*. In each case, an increase in LF concentration monotonically decreases the PA_{63} current for $V > 0$.

To estimate the apparent binding constant of LF to the PA_{63} pore, we assume that one LF molecule binds reversibly to the channel (21) and can thereby block it. A least squares best fit of this simple model to the data in Fig. 2*E* suggests that the apparent dissociation constant is $K_D \sim 50$ pM. Despite the good fit of the model to the data, LF may bind even more strongly to PA_{63}. For example, the actual concentration of LF might be lower if LF binds to trace amounts of PA_{63} (~10 pM) in solution. The apparent binding constant deduced from the effect of LF on the PA_{63} channel *I-V* relationship (Fig. 2*E*) is consistent with estimates from cell-based and Biacore surface plasmon resonance (SPR) assays (~10 pM to 2.5 nM) (22–24). However, unlike SPR, the electrophysiology method described here provides a functional test of PA_{63} and LF and is obtained in minutes rather than days as is required by cell-based methods.

Although we do not yet understand the physical mechanism for EF- and LF-induced rectification of the PA_{63} channel, the schematic in Fig. 2*F* illustrates several hypothetical models for the effect. There are at least two possible mechanisms that can account for the LF-induced current decrease for $V > 0$ (Figs. 1 and 2). LF could be forced into the pore entrance, perhaps by the small electric field gradient near the pore mouth, and thereby occlude the channel (Fig. 2*F*, *top panel*). Alternatively, LF might be driven completely through the channel (not illustrated). EF or LF channel blockade reversal by negative potentials may be the result of their removal from the PA_{63} ion conduction pathway like a swinging gate or the complete separation from the PA_{63} channel (Fig. 2*F*, *bottom panel*).

The $(PA_{63})_7$-LF interaction (Fig. 2) might prove useful for understanding the mechanism by which PA, LF, and EF traverse the endosomal membrane through further characterization of the protein-protein interactions. Another promising prospect includes identifying and screening compounds and/or antibodies that disrupt toxin function or interaction. To test this hypothesis, we use a previously characterized monoclonal antibody, 1G3–1-1, that prevents binding of LF to PA_{63} through steric hindrance (9). Briefly, previous studies showed that 1G3–1-1 neutralized LF toxin both *in vivo* and *in vitro*. *In vivo*, this monoclonal antibody protected 100% of animals injected with lethal toxin (*i.e.* LF bound to the PA_{63} heptamer). *In vitro*, the monoclonal antibody prevented LF from binding to the protective antigen and neutralized the cytolytic activity even if lethal toxin was formed prior to monoclonal antibody addition (9). Although it is known that this antibody inhibits the binding of LF to PA, to date there have been no reported studies showing the effect of antibodies on the channel conductance. In our

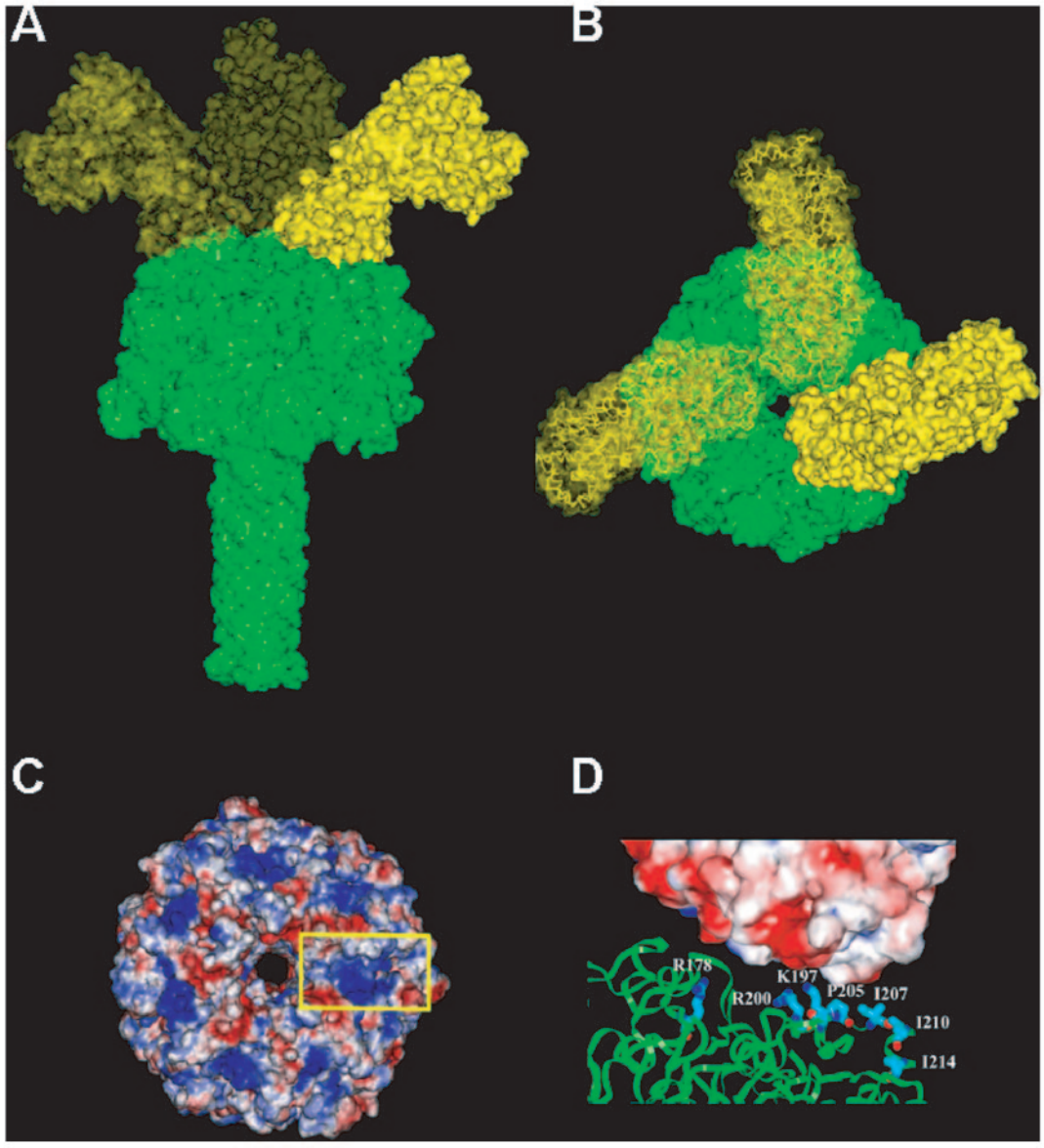

FIGURE 4. **Molecular models of the PA_{63} heptamer and the PA_{63} heptamer-LF complex.** The proteins are shown as surface renderings. The pore model is based on theoretical work by Nguyen (27). The LF rendering is from the crystal structure determined by Pannifer *et al.* (35) (PDB code 17JN) and mapping of the LF binding site by others (9, 21, 33, 34). *A* and *B*, side and top views of PA_{63} heptamer (*green*) bound to three LF molecules (*yellow*). *C* and *D*, the surface renderings are colored according to the negative (*red*) and positive (*blue*) electrostatic surface potential. *C*, top view of the PA_{63} heptamer. The *yellow box* highlights the protomer-protomer interface and where LF binds to heptameric PA. *D*, a hypothetical PA_{63} heptamer-LF interface. LF is shown as a surface rendering; PA is rendered in *green ribbon*. The residues that have been mapped as part of the LF binding site are shown as *thick sticks* (carbon atoms colored *cyan*, oxygen atoms *red*, and nitrogen atoms *blue*). In this model, the positive surface potential of the LF binding site in the PA_{63} heptamer is matched to the negative surface potential of LF at its PA binding site.

electrophysiological studies, the antibody had virtually no effect on the *I-V* relationship of PA_{63} channels but completely inhibited LF-induced blockade (Fig. 3*A*). As a control, incubating the channels with bovine serum albumin (150 nM) had no effect on LF-induced PA_{63} channel blockade (data not shown). Thus, the effect of the antibody is specific. We conclude that the results in Fig. 3*A* provide the basis for a quantitative biosensor to rapidly screen for one type of anthrax therapeutics. Agents that bind to the PA_{63} channel (and do not cause current blockades) or to LF would inhibit LF-induced rectification of the instantaneous *I-V* relationship for PA_{63} channels. Other potentially useful anthrax therapeutics could conceivably bind to and occlude the PA_{63} pore.

In a recent study, we showed the presence of a functionally active complex in the serum of infected animals (14). To demonstrate the applicability of this method for diagnostic purposes, we first characterized the channel properties of anthrax lethal toxin complex purified from the serum of an infected guinea pig. Serum samples contain a large number of contaminating cellular and bacterial proteins that may possibly interfere with the channel recordings. Hence, size exclusion chromatography was used to remove most of the small contaminating proteins, although the fraction corresponding to the high molecular weight complex may also contain some contaminating proteins. The purified *in vivo* $(PA_{63})_7$-LF complex, at an initial LF concentration of ~30 pM in the bilayer chamber, formed strongly rectifying channels (Fig. 3, *B* and *C*), as do PA_{63} channels after the addition of LF (*e.g.* Fig. 2*D*) and the complex formed *in vitro* (14). These results clearly demonstrate the physiological relevance of the rectifying channel *in vivo*. In addition, they support earlier results that suggested that PA_{63} was complexed with lethal factor in the blood of infected animals (25). The concentration and activity of

LF in the *in vivo* formed complex was determined using a fluorescent-based kinetic assay (Fig. 3*D*) as described under "Experimental Procedures." Having identified and characterized the conducting properties of the purified infected complex, we may eventually be able to isolate the signal of the complex from the noise generated by contaminating serum proteins. Studies are ongoing to detect the complex in serum samples at various stages of infection.

Figs. 1–3 demonstrate that LF and EF bind to and block the PA_{63} channel at positive applied potentials. This observation raises the question: why is the PA_{63} channel blocked only at positive potentials? Recent experiments (26) and molecular modeling (27) indicate that the $(PA_{63})_7$ channel bears a striking similarity to the crystal structure of the *S. aureus* α-hemolysin channel (28). According to the model for the PA_{63} channel, it has a mushroom-shaped cap domain and a long stem (Fig. 4, *A* and *B*) that consists of 14 strands that comprise an anti-parallel β-barrel. The model illustrates how three LF molecules might bind to the PA_{63} channel. Because the LF- and EF-induced blockades are sensitive to electric field polarity, it is reasonable to speculate that an electrostatic or electrokinetic mechanism is involved. The LF binding site on the PA_{63} channel is mostly basic (Fig. 4*C*); it is possible that when the transmembrane potential polarity is reversed, the net positive or negative surface charges of the LF molecule (Fig. 4*D*) cause small mechanical shifts in its position, resulting in PA_{63} channel blockade.

Based on this hypothetical model, the blockade of the channel by LF for positive applied potentials could be caused by either a physical occlusion (by LF) or a change in the PA_{63} channel structure induced by the binding of LF. The view shown in Fig. 4*B* suggests that even a small shift in the location of a single LF molecule could block the pore entrance. It is conceivable that a positive (or negative) potential would drive LF into (or out of) the ionic conduction pathway as discussed above.

Because the LF-induced block of the PA_{63} channel can be triggered by very small positive potentials or removed by very small negative potentials, the portion of LF that occludes the pore may lie close to or be attached to the pore mouth at all times. For example, we found that when a steady membrane potential is reversed from negative to positive polarity (50 mV) in the presence of LF at $\sim 2 \times 10^{12}$ molecules/cm^3 (Fig. 1), the occlusion occurs in less than 50 ms with no subsequent increase in current (data not shown). Simple but conservative model calculations indicate that this rapid occlusion cannot be explained by the LF flux arriving at the channel entrances via diffusion from the bulk (<2 LF molecules/s) or by LF molecules being driven there by the small electric field ($\sim 5 \times 10^{-9}$ V/cm) in the bulk electrolyte solution. The slightly reduced ionic current for negative membrane potentials observed in the presence of LF (Fig. 1) would also be consistent with LF strongly bound near the channel openings but only partially blocking the ionic current. Additional experimental results and analysis are needed to determine the mechanism by which the applied potential modulates the LF-induced PA_{63} current blockages.

Electrophysiology measurements of PA_{63} channel blockade by EF_N (18) and LF_N (19) and cell-based studies that demonstrate the LF- and LF_N-induced blockade of PA_{63}-doped cells (20) have led to the hypothesis that at pH 5.5 LF and EF are translocated through PA_{63} channels that have a diameter of ~1.1 nm (16, 17). Our results using the physiologically relevant full-length LF at pH 6.6 show that the LF-induced PA_{63} current blockades are persistent (Fig. 1). The blockades remain even after extensive perfusion and the passage of more than 20 min (data not shown). The blockade is neither short-lived nor removed by an increase in transmembrane potential (Figs. 1 and 2). In addition, there are no observed short-lived transient blockades caused by LF at pH 6.6. It has been shown that the passage of individual polynucleotides through the α-hemolysin channel causes transient current blockades (29, 30) and that proteins can occlude other channels (31). Thus, most likely, the full-length LF does not thread through the channel at pH 6.6. Our data support the model depicted in Fig. 2*F* that shows LF bound to PA_{63} for long times and that it acts as a gate that is open for negative voltages and closed for positive voltages.

Our preliminary experiments at pH 5.5 suggest that full-length LF does not bind as strongly to the PA_{63} channel as it does at pH 6.6. However, none of those data suggest that the full-length LF translocates through the PA_{63} pore. Several key differences in our approach as compared with that in a recent report (19) are the pH (6.6), which affects the value of fixed charges on the protein surfaces, the larger size of the physiologically relevant full-length LF and EF (*e.g.* 89 kDa *versus* 30 kDa for EF_N), and the use of instantaneous *I-V* data.

In this report, electrophysiological measurements and analysis of the functional interaction between anthrax toxins in planar bilayer membranes demonstrate that LF and EF bind to the PA_{63} channel and convert it to a strongly rectifying pore at pH 6.6. At ~10 pM concentration, LF occludes PA_{63} channels in planar lipid bilayer membranes for $V > 0$. The marked voltage-dependent, diode-like effect suggests that PA may control the direction of ion flow across cell membranes. The toxins may also influence the transmembrane potential, as is true for other rectifying channels (for review see Ref. 32). By controlling the endosomal pH and H^+ influx, PA could create an ideal environment for toxin translocation and/or lysis of the endosome. Exploitation of this effect as an innovative means of characterizing anthrax toxin interactions is only one demonstration of the value of this technique. In comparison to other methods, such as monoclonal antibody assays measuring competition between radiolabeled LF and unlabeled LF or EF to PA (22), cell-based cytotoxicity assays (23), and surface plasmon resonance measurements (24), the approach reported here is a rapid quantitative tool to determine the effective concentrations/binding constants or disruption between LF or EF with PA_{63}. This report demonstrates three exciting applications of this method as a biosensor for anthrax diagnostics. First, full-length LF or EF can be rapidly quantitated at low concentrations. Second, therapeutic agents against anthrax can be rapidly screened. Third, purified lethal toxin from infected animal blood can be detected at low concentrations (~30 pM). The application of the methods described herein will enhance efforts to render anthrax toxin ineffective.

Acknowledgments—We thank Dr. John Ezzell and Wilson Ribot (U. S. Army Medical Research Institute of Infectious Diseases) for the kind gift of the purified $(PA_{63})_7$-LF complex from infected animals.

REFERENCES

1. Inglesby, T. V., O'Toole, T., Henderson, D. A., Bartlett, J. G., Ascher, M. S., Eitzen, E., Friedlander, A. M., Gerberding, J., Hauer, J., Hughes, J., McDade, J., Osterholm, M. T., Parker, G., Perl, T. M., Russell, P. K., and Tonat, K. (2002) *J. Am. Med. Assoc.* **287,** 2236–2252
2. Bradley, K. A., Mogridge, J., Mourez, M., Collier, R. J., and Young, J. A. (2001) *Nature* **414,** 225–229
3. Scobie, H. M., Rainey, G. J., Bradley, K. A., and Young, J. A. (2003) *Proc. Natl. Acad. Sci. U. S. A.* **100,** 5170–5174
4. Molloy, S. S., Bresnahan, P. A., Leppla, S. H., Klimpel, K. R., and Thomas, G. (1992) *J. Biol. Chem.* **267,** 16396–16402
5. Klimpel, K. R., Molloy, S. S., Thomas, G., and Leppla, S. H. (1992) *Proc. Natl. Acad. Sci. U. S. A.* **89,** 10277–10281
6. Petosa, C., Collier, R. J., Klimpel, K. R., Leppla, S. H., and Liddington, R. C. (1997) *Nature* **385,** 833–838
7. Mourez, M., Lacy, D. B., Cunningham, K., Legmann, R., Sellman, B. R., Mogridge, J., and Collier, R. J. (2002) *Trends Microbiol.* **10,** 287–293
8. Milne, J. C., and Collier, R. J. (1993) *Mol. Microbiol.* **10,** 647–653
9. Little, S. F., Novak, J. M., Lowe, J. R., Leppla, S. H., Singh, Y., Klimpel, K. R., Lidgerding, B. C., and Friedlander, A. M. (1996) *Microbiology* **142,** Pt. 3, 707–715

10. Little, S. F., Leppla, S. H., and Cora, E. (1988) *Infect. Immun.* **56,** 1807–1813
11. Montal, M., and Mueller, P. (1972) *Proc. Natl. Acad. Sci. U. S. A.* **69,** 3561–3566
12. Kasianowicz, J. J., and Bezrukov, S. M. (1995) *Biophys. J.* **69,** 94–105
13. Panchal, R. G., Hermone, A. R., Nguyen, T. L., Wong, T. Y., Schwarzenbacher, R., Schmidt, J., Lane, D., McGrath, C., Turk, B. E., Burnett, J., Aman, M. J., Little, S., Sausville, E. A., Zaharevitz, D. W., Cantley, L. C., Liddington, R. C., Gussio, R., and Bavari, S. (2004) *Nat. Struct. Mol. Biol.* **11,** 67–72
14. Panchal, R. G., Halverson, K. M., Ribot, W., Lane, D., Kenny, T., Abshire, T. G., Ezzell, J. W., Hoover, T. A., Powell, B., Little, S., Kasianowicz, J. J., and Bavari, S. (2005) *J. Biol. Chem.* **280,** 10834–10839
15. Blaustein, R. O., and Finkelstein, A. (1990) *J. Gen. Physiol.* **96,** 943–957
16. Blaustein, R. O., Lea, E. J., and Finkelstein, A. (1990) *J. Gen. Physiol.* **96,** 921–942
17. Blaustein, R. O., and Finkelstein, A. (1990) *J. Gen. Physiol.* **96,** 905–919
18. Finkelstein, A. (1994) *Toxicology* **87,** 29–41
19. Zhang, S., Udho, E., Wu, Z., Collier, R. J., and Finkelstein, A. (2004) *Biophys. J.* **87,** 3842–3849
20. Zhao, J., Milne, J. C., and Collier, R. J. (1995) *J. Biol. Chem.* **270,** 18626–18630
21. Singh, Y., Klimpel, K. R., Goel, S., Swain, P. K., and Leppla, S. H. (1999) *Infect. Immun.* **67,** 1853–1859
22. Leppla, S. H. (1991) in *Sourcebook of Bacterial Protein Toxins* (Alouf, J., ed) pp. 277–302, Academic Press, New York
23. Quinn, C. P., Singh, Y., Klimpel, K. R., and Leppla, S. H. (1991) *J. Biol. Chem.* **266,** 20124–20130
24. Elliott, J. L., Mogridge, J., and Collier, R. J. (2000) *Biochemistry* **39,** 6706–6713
25. Ezzell, J. W., Jr., and Abshire, T. G. (1992) *J. Gen. Microbiol.* **138,** 543–549
26. Benson, E. L., Huynh, P. D., Finkelstein, A., and Collier, R. J. (1998) *Biochemistry* **37,** 3941–3948
27. Nguyen, T. L. (2004) *J. Biomol. Struct. Dyn.* **22,** 253–266
28. Song, L., Hobaugh, M. R., Shustak, C., Cheley, S., Bayley, H., and Gouaux, J. E. (1996) *Science* **274,** 1859–1866
29. Kasianowicz, J. J., Brandin, E., Branton, D., and Deamer, D. W. (1996) *Proc. Natl. Acad. Sci. U. S. A.* **93,** 13770–13773
30. Kasianowicz, J. J., Henrickson, S. E., Weetall, H. H., and Robertson, B. (2001) *Anal. Chem.* **73,** 2268–2272
31. Simon, S. M., and Blobel, G. (1991) *Cell* **65,** 371–380
32. Lu, Z. (2004) *Annu. Rev. Physiol.* **66,** 103–129
33. Chauhan, V., and Bhatnagar, R. (2002) *Infect. Immun.* **70,** 4477–4484
34. Cunningham, K., Lacy, D. B., Mogridge, J., and Collier, R. J. (2002) *Proc. Natl. Acad. Sci. U. S. A.* **99,** 7049–7053
35. Pannifer, A. D., Wong, T. Y., Schwarzenbacher, R., Renatus, M., Petosa, C., Bienkowska, J., Lacy, D. B., Collier, R. J., Park, S., Leppla, S. H., Hanna, P., and Liddington, R. C. (2001) *Nature* **414,** 229–233